Ice-Templated Structures for Biomedical Tissue Repair: from Physics to Final Scaffolds

K. M. Pawelec, A. Husmann, S. M. Best, R. E. Cameron

April 16, 2014

Ice-templating techniques, including freeze-drying and freeze casting, are extremely versatile and can be used with a variety of materials systems. The process relies on the freezing of a water based solution. During freezing, ice nucleates within the solution and concentrates the solute in the regions between the growing crystals. Once the ice is removed via sublimation, the solute remains in a porous structure which is a negative of the ice. As the final structure of the ice relies on the freezing of the solution, the variables which influence ice nucleation and growth alter the structure of ice-templated scaffolds. Nucleation, the initial step of freezing, can be altered by the type and concentration of solutes within the solution, as well as the set cooling rate before freezing. After nucleation, crystal growth and annealing processes, such as Ostwald ripening, determine the features of the final scaffold. Both crystal growth and annealing are sensitive to many factors including the set freezing temperature and solutes. The porous structures created using ice-templating allow scaffolds to be used for many diverse applications, from microfluidics to biomedical tissue engineering. Within the field of tissue engineering, scaffold structure can influence cellular behavior, and is thus critical for determining the biological stimulus supplied by the scaffold. The research focusing on controlling the ice-templated structure serves as a model for how other ice-templating systems might be tailored, to expand the applications of ice-templated structures to their full potential.

Contents

1 Introduction

The phase transition from water to ice is one which often occurs in the daily world around us. In fact, the transition from water to ice is unique in several ways and a process which continues to fascinate scientists in its complexity. At normal pressures, ice exists as a hexagonal crystal structure which is held together via hydrogen bonding [1]. In comparison to the disordered liquid, molecules within the crystal structure of the solid are further apart, causing the density of ice to decrease during the transition from a liquid to a solid [1]. As the structure of ice forms, it has a tendency to exclude impurities or solutes rather than incorporating them into the crystal lattice [1]. Thus, ice is "self-cleaning" and solidification results in the spaces between ice grains being enriched in solutes. The self-cleaning nature of ice makes it useful for a number of applications, such as purifying solutes and creating porous structures, both of which are accomplished through a broad technique called ice-templating.

1.1 Ice-Templating

The term ice-templating applies to any technique which utilizes ice to form a three-dimensional structure, such as freeze-drying and freeze casting. During the ice-templating process, ice nucleates within a solution. As it grows it excludes solute, and when subsequently removed via sublimation, only a porous structure, which mirrors the ice crystal structure, remains. The ice-templating technique is versatile, and has been used with a variety of materials systems: from polymers to colloids and ceramics [2–4].

The end product of ice-templating is a porous material, with a structure that can be either isotropic or anisotropic. The pore size can range from several hundred micrometers down to fine structures of less than 1 μm, depending on the way in which solidification occurs. The wide range of structures adds to the versatility of the technique. By controlling the pore structure, macroscopic properties, such as mechanical strength or surface area of the scaffolds, can be fine tuned [5]. Tailoring the scaffold structure requires the control of ice nucleation and growth. It is therefore important to understand the physics of ice solidification and the many variables which can be altered during the process.

1.2 Biomedical Applications for Ice-Templated Structures

Applications of ice-templated structures are numerous. Not only can these structures be used in diverse technologies such as microfluidics and continuous flow catalysts, but biomedical tissue engineering scaffolds also require well defined porous structures to allow tissue regeneration [6–8]. Within biomedical applications, scaffold structure influences cellular behavior through architectural cues such as pore size, isotropy, and inter-connectivity, all of which can be controlled in ice-templating [8–10].

There are many types of polymeric biomaterials scaffolds, including synthetic polymers such as polylactide-co-glycolide (PLGA), and natural polymers, such as chitosan and collagen [11]. Of the many natural polymers possessing inherent biocompatibility, collagen, the natural structural component within the body is ideal as a tissue engineering scaffold. Not only is collagen biocompatible, but it can interact with a number of molecules normally found within the ECM, such as hyaluronic acid and growth factors, such as insulin-like growth factor 1 [12, 13]. The mechanical properties of the material, important for guiding the biological interactions of cells on scaffolds, depend on the scaffold composition and chemical modifications, such as cross-linking [14–16]. Within the body, collagen is made as fibers, and scaffolds of collagen fibers have been used for applications such as tendon and ligament tissue engineering [17, 18]. Collagen scaffolds made from ice-templating have advantages over fibers for their ability to encourage cell infiltration via an interconnected porous structure [9]. However, the two types of collagen scaffolds can also be combined to create fiber reinforced scaffolds [19]. Thus far,

the clinical outcomes for collagen biomedical scaffolds are encouraging, and diverse. It has been shown that collagen scaffolds form an ideal network for creating *in vitro* models of tissue, such as the mammary gland [20]. For the repair of the cartilage and bone interface in joints, mineralized collagen scaffolds have also demonstrated good clinical results, and are currently used as a viable therapy within regenerative medicine [21–23].

While chemical composition and mechanical properties are important for determining biological response to tissue engineering scaffolds, architectural cues also play an important role. Scaffold structure can be described by the pore size and the isotropy, or directionality, of the pores. Both factors affect cell response. Scaffold pore size has been shown to affect cell adhesion which can alter the long-term outcome of tissue engineering constructs [9]. On the other hand, many natural tissues possess an extra-cellular matrix with an inherent anisotropic structure which allows them to perform their biological function. Tendon, for example, is composed of aligned collagen bundles oriented parallel to the mechanical load [24]. Indeed, anisotropic scaffolds which allow tendon cells to elongate, encourage a more characteristic phenotype [25–27]. Through the use of specialized molds, scaffold isotropy can also be altered to mimic natural tissues using ice-templating [10, 28]. As key features of scaffold structure, both anisotropy and pore size must be fine-tuned for biomedical applications, and the process is intimately related to the physics surrounding the ice solidification process [29, 30].

1.3 Outline of Review

The process of ice solidification can be broken up into two processes: nucleation and crystal growth. Both phases of solidification impact the porous structure created through the use of ice-templating. Thus, a portion of the review will focus on the crystallization of ice and how the process is controlled, starting with an overview of nucleation.

At nucleation water molecules come together to form the first solid, which will then be subject to crystal growth. Nucleation is stochastic by nature, and therefore can never be completely controlled, although methods exist, such as addition of nucleation agents, which can narrow the range of temperatures at which nucleation occurs [31]. While the nucleation event may be stochastic, it is influenced by many different parameters including whether nucleation is homogeneous or heterogeneous, solute additions and the set cooling rate of the system.

Once nucleation has occurred, crystal growth takes over. During the initial conversion of liquid to a solid, the rate of crystal growth in ice is sensitive to both the heat flow within the system and the solutes present. Even after all of the available liquid has been converted into a solid, the scaffold structure continues to evolve. The remodeling of the ice structure below the equilibrium freezing temperature (0°C) is a universal feature of ice solidification and is again dependent on many factors, such as temperature, time and composition of the solution.

Having examined ways in which ice solidification can be controlled, the impact on scaffold structure in ice-templating will be defined for biomedical applications. In particular, the focus is on biopolymer scaffolds for use in biomedical applications. While ceramics applications are not within the scope of this review, they have been previously addressed by Deville [32]. Biopolymer scaffolds are playing a critical role in tissue engineering for their open, interconnected pore structure which can be tuned to influence cellular behavior. As the scaffold structure is critical for controlling cell interactions, it is important to understand the ice-templating process in order to tailor scaffolds to specific biomedical application [8]. As freezing is intimately associated with the set freezing protocol used during solidification, there has been a focus in the literature on using the set freezing protocol to control scaffold structure. Aspects such as the set freezing temperature, the set cooling rate, and the addition of thermal holds are all ways in which to manipulate the final structure, and ultimately the biological properties of biopolymer scaffolds.

2   Nucleation

The process of solidification, otherwise known as freezing, begins with the initial nucleation of a crystal, called a nucleus. There exists a barrier to the formation of stable nuclei due to several factors: the inherent lowering of entropy within the system by replacing a liquid with an ordered solid, the increased strain energy, and the increased inter-facial energy at the solid-liquid interface [33]. Thus, while all systems have an equilibrium temperature of freezing, stable nuclei rarely, if ever, form at that temperature [33, 34]. Instead, liquid systems exist in a metastable state below the freezing temperature, with clusters of molecules in an ordered structure, but with no long range order, Figure 1 [34–36].

Once the small clusters of molecules grow large enough, stable bonds are formed, releasing excess energy in the form of latent heat [33, 34]. The temperature at which this occurs is called the nucleation temperature. The difference between this temperature and the equilibrium temperature is defined as undercooling, also called supercooling [33, 34]. As nucleation temperature decreases, the size of a stable nucleus within pure ice-water systems decreases as well [37]. The excess energy released, termed the latent heat, flows into the liquid surrounding the stable nuclei, raising the temperature of the surrounding environment [34]. The initial nucleation event, termed primary nucleation, releases latent heat, the amount of which is related to the volume of liquid converted to a solid [33]. After primary nucleation, any further nuclei which form are part of a process called secondary nucleation. [33].

It is generally acknowledged that the final structure of the solid, whether isotropic or anisotropic, is determined by the nucleation step. Thus nucleation is an important target to control scaffold architecture, which mirrors ice crystal structure [38, 39]. When a solution is cooled in such a
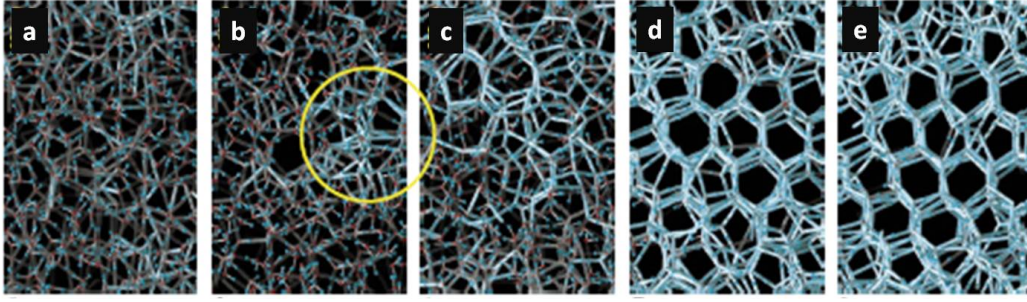
Figure 1: A computer simulation of the solidification of water at time (a) 208 ns, (b) 256 ns (c) 290 ns, (d) 320 ns, and (e) 500 ns. After an initial nucleus forms, the circled region in (b), longer lasting hydrogen bonds begin to form around it until the entire liquid has been replaced with an ordered crystal structure. [35] Reprinted by permission from Macmillan Publishers Ltd: Nature, 416(6879), 409 (2002). Copyright 2002.

Table 1: Variables which affect nucleation temperature

Variable	Example System	Influence on Nucleation Temperature	Reference
Nucleating Agents	0.001 wt/vol% *Pseudomonas syringae*, 1% silver Iodine (AgI)	addition of agents	[41, 42]
	10% iron ore, 10% river sand	***increased*** temperature	[42]
Solute size	0.2-3.4µm alumina particles (28 vol%)	decreased size, ***increased*** temperature	[43]
Solute type	0.3µm alumina (32 vol%) with 0.2-1wt% sodium polymethacrylate	increased sodium ions, ***decreased*** temperature	[44]
Set Cooling Rate	0.05 - 5 °C/min; 1-3 mm diameter water droplet	increased set cooling rate, ***increased*** temperature	[45]
	0.05 - 1 °C/min; 2ml of 10wt% hydroxyethyl starch	no change	[46]

way that stable undercooling is achieved throughout, nucleation and the accompanying crystal growth occurs within the entire volume [38]. However, in non-equilibrium systems, only a small volume may achieve sufficient undercooling and nucleate. After the initial nucleation occurs, the remaining liquid is frozen by ice crystal growth, as seen in Figure 2 [38]. For this reason, control over nucleation is of great importance during freezing and several variables are known to affect it, summarized in Table 1.

2.1   Mechanism of Primary Nucleation

While the equilibrium freezing temperature of ice is 0 °C, the nucleation temperature reached before stable nuclei form can vary from around 0 °C to -40 °C in special systems [33]. The variation is linked to the amount of energy required to form a stable nucleus, which is partially dictated by the method of nucleation [33]. Homogeneous nucleation requires a high driving force to offset the additional energy of creating a new solid-liquid interface in pure ice-water
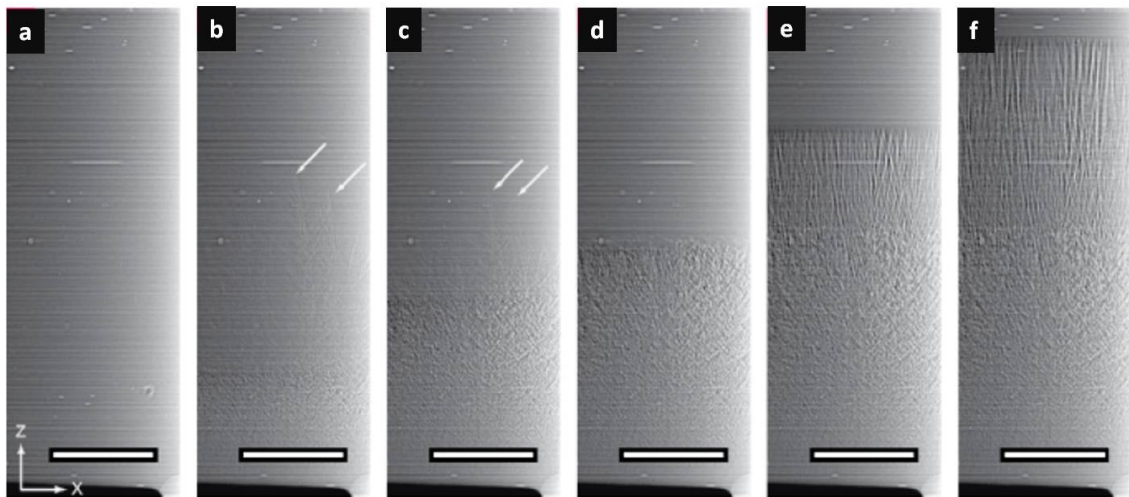
Figure 2: The evolution of crystal structure upon directional solidification of a colloidal alumina suspension. The structure was viewed using x-ray tomography at time (a) 50, (b) 51, (c) 52.1, (d) 53.6, (e) 59.7, and (f) 516.3 seconds. Scale bar: 500 mm. White arrows point to fast growing crystals, while the black base is a copper surface [40]. Reproduced with permission from J. Am. Ceram. Soc., 92 [40] 2489–2496 (2009). Copyright 2009 The American Ceramic Society.

systems [33]. Thus, the lowest nucleation temperatures, around -40 °C in ultra-pure water droplets, are found in water where all contaminants have been thoroughly removed [33]. Heterogeneous nucleation occurs where critical sized nuclei form at an impurity interface, which can include mold walls, or solutes [33]. Heterogeneous nucleation is responsible for the majority of solidification, and allows nucleation to take place with a much smaller undercooling, as the energy of creating a new solid-liquid interface is offset by the inter-facial energy existing between the surface and the nuclei [33].

Nucleation, whether homogeneous or heterogeneous, is a stochastic process [31]. Even when the exact same sample is refrozen, the nucleation temperature can vary by several degrees [31]. The stochastic nature of ice nucleation means that at every nucleation temperature, there exists a probability of ice nucleating. In reality, this leads to a delay in nucleation at a given temperature. At an undercooling of 8 degrees, an average delay of 1000 - 3000 seconds occurs before nucleation is initiated, which was reduced with larger undercooling [47]. Within pure ice-water systems, it has been found that the amount of undercooling depends on the sample volume; larger volumes of water raise the nucleation temperature [38, 39, 42, 45].

2.2 Mechanism of Secondary Nucleation

The relative rarity of primary nucleation events, and the considerable lag time between events, means that primary nucleation is not responsible for every grain formed at nucleation. Instead, a phenomenon known as secondary nucleation plays an important role in the final crystal
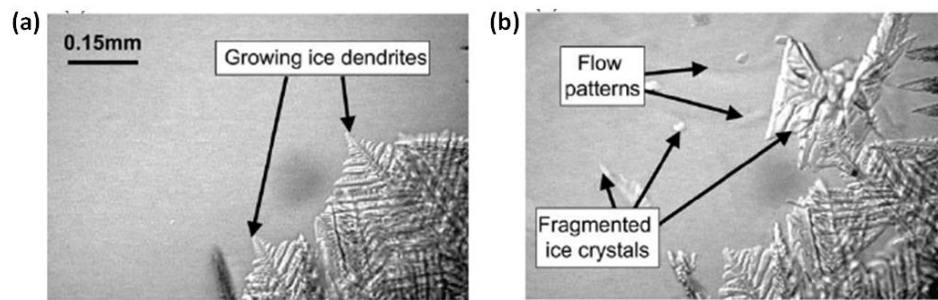
Figure 3: Secondary nucleation from dendrite fragments produced via ultrasound in a 15 wt% sucrose solution. Ice dendrites were clearly visible (a) before ultrasound, and (b) after 1.36 seconds of ultrasound, flow patterns and fragments of ice dendrites were visible in the liquid [48]. Reprinted from Ultrasonics, 41(8), Chow R, Blindt R, Chivers R, Povey M, The sonocrystallisation of ice in sucrose solutions: primary and secondary nucleation, 595-604, Copyright (2003), with permission from Elsevier.

structure, although the kinetics and root cause are not yet completely clear [33]. In secondary nucleation, crystals originating from a parent crystal are dispersed within the liquid, and act as new sites for crystal growth, forming new grains of ice [48]. Any process which results in the shearing of ice crystal fragments from a parent crystal increases secondary nucleation, Figure 3 [48]. Several possible mechanisms, besides shearing of primary crystals, are believed to contribute to secondary nucleation including high local concentrations of solute in the liquid phase and uneven convection currents [33, 49].

2.3   The Effect of Solute Addition

The dominant mechanism of primary nucleation is heterogeneous nucleation. The presence of solutes and polymers within pharmaceutical solutions and collagen suspensions influence not only the crystal growth of ice, but change nucleation. Nucleation agents are an extreme case of controlling nucleation via additives. They are used to increase the probability that nucleation will occur within a narrow temperature range [41, 42]. Common nucleation agents in pharmaceutical literature include silver iodide (AgI) and *Pseudomonas syringae*; however nucleation agents within nature vary widely and can range from iron ore to river sand [41, 42]. The mechanism by which nucleation agents act varies; a few, like silver iodide, have a crystal structure which closely resembles ice and can act as a template for ice crystal formation, while the majority of nucleation agents depend upon surface roughness to initiate nucleation [42].

In most cases, the effect of solutes, such as sucrose or nanoparticles, is not as marked as that observed with nucleation agents. In dilute solutions, solutes can decrease the saturated vapor pressure of the solution, via Raoult's law, which results in lowering the freezing temperature [34]. It has been noted experimentally, within aqueous systems, that larger ice crystals are formed with smaller solutes, an effect contributed to the increased surface area of solute which

can participate in nucleation reactions [43, 50]. An increase in surface area per unit volume provides more nucleation sites, thus catalyzing the nucleation of ice at higher temperatures, leading to larger ice crystals [43]. Higher concentrations of solutes lower the nucleation temperature and generally yield smaller ice crystals than low concentrations [50]. At high enough concentrations, solutes may inhibit the formation of crystalline ice altogether [50].

The type of solute can also affect nucleation. For example, ionic solutes interfere with nucleation, while non-ionic solutes, such as glucose, glycerol and nanoparticles have a less dramatic effect [44, 51]. Within collagen suspensions, both large polymers and small acidic solutes are present and both may contribute to the nucleation of the suspension.

2.4   The Effect of Cooling Rate

While the changes to ice nucleation with solute addition, are relatively straightforward, the dependence of nucleation temperature on the set cooling rate is much harder to unravel. When considering the method of freezing and the effects on nucleation, a distinction must be made between variables which can be directly controlled, defined as "set" , and those which occur locally within samples and are indirectly controlled. For example, the "set" cooling rate refers to the rate at which a sample is cooled from an external source, whereas the cooling rate of the sample is due entirely to heat flow in and around the specific volume of interest. In turn, a distinction must also be made between the set cooling rate, defined here as the rate of cooling applied to a system before nucleation, and the freezing rate, or the rate of ice crystal growth after nucleation which cannot be directly controlled [52]. Within the literature, no universal definition exists, and freezing rate and cooling rate are sometimes used interchangeably.

Many different methods exist to cool samples, such as shelf ramping and quenching [52]. Ice nucleation temperature can be influenced by the freezing technique,which differ in respect to the applied cooling rates and heterogeneities in temperature which are introduced within samples [52]. Thus, the cooling rate effect is difficult to separate out, though various groups have reported on it. When water droplets did not exceed 1mm in diameter, lowering the set cooling rate from 0.05 °C/min to 0.5 °C/min resulted in a higher nucleation temperature, on the order of 1-2 degrees [45]. However, when studying the freezing of 2 ml of 10 wt% (w/v) hydroxyethyl starch (HES) solution, it was found that moderate set cooling rates of between 0.05 and 1 ℃/min had no effect on the nucleation temperature [46].

3   Crystal Growth

Once nuclei have formed, their size and shape is affected by the crystal growth. The formation of porous structures, such as tissue engineering scaffolds, requires a disturbance of the solid-liquid interface [53]. Perturbations leading to porous structures can occur from secondary
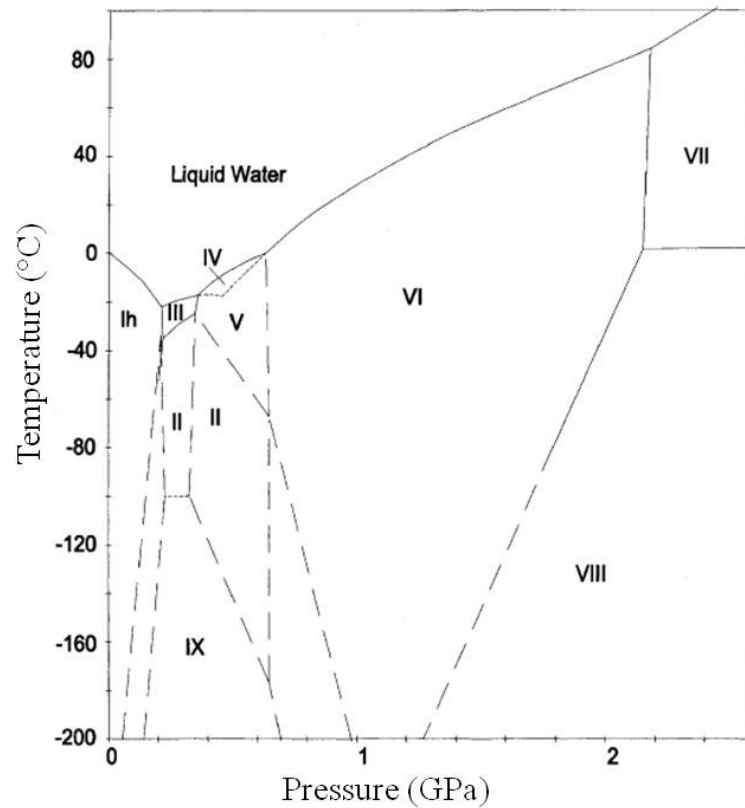
Figure 4: The phase diagram of ice. Under normal conditions, ice is in a Ih form, however, many possible structures exist [34]. Reprinted from Energy Conversion and Management 43 (2002), M Akyurt, G Zaki, B Habeebullah, Freezing phenomena in ice–water, 1773–1789, Copyright (2002), with permission from Elsevier.

nucleation events, temperature inhomogeneities and non-equilibrium solute distribution in the region of the solid-liquid front [53, 54]. Like nucleation, crystal growth can be affected by many variables, which are summarized in Table 2.

Many different ice crystal structures exist, especially at low temperatures and very high pressures, Figure 4 [1, 34]. At normal temperatures and physiological pressures, ice occurs in the Ih form, which is described by a hexagonal unit cell [1]. Three a-axes, separated by 120°, lie within a plane, which is orthogonal to the c-axis, Figure 5 [1]. Adding molecules onto the a-axis requires the formation of fewer bonds than adding molecules to the c-axis. The result is that crystal growth occurs 10^2- 10^3 times faster along the a-axes compared with the c-axis [1].

3.1   Crystal Growth Kinetics

The kinetics of crystal growth are dictated by several factors, including temperature, heat flow, and solutes. The growth rate increases rapidly as the temperature moves below equilibrium [36, 55, 57]. The environment also affects the rate of growth by governing how efficiently the latent heat is removed [57]. A decrease of 1 degree, from -1 to -2 °C, can increase the growth
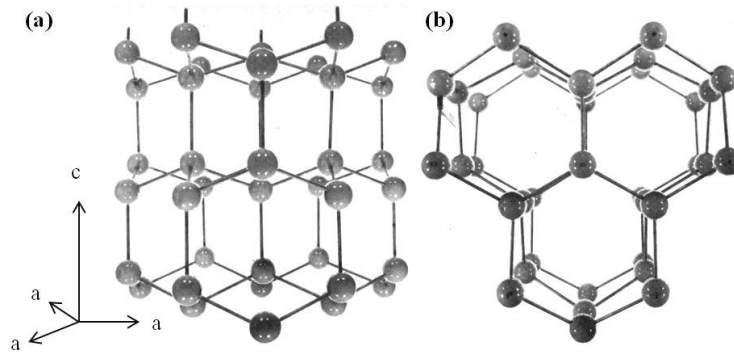
Figure 5: The structure of oxygen atoms within Ih ice with hydrogen bonds represented as rods [1]. (a) Perpendicular to the c-axis and (b) parallel to the c-axis. Ice Physics by Hobbs (1974). By permission of Oxford University Press.

Table 2: Factors which affect the ice crystal growth rate

Variable	Example System	Influence on Crystal Growth Rate	Reference
Set Freezing Temperature	0.1-1 ml water droplet; frozen at 0 to -25ºC	decreased temperature,	[55]
	20% sucrose solution; 0 to -15ºC	***increased*** growth rate	[56]
Thermal Conductivity	water droplets frozen on glass or brass plate	increased thermal conductivity, ***increased*** growth rate	[57]
Crystal Orientation	a-axis vs c-axis	a-axis (the kinetically favorable plane) grows faster	[40,58]
Solute Size	> 125 µm titanium particles	no porosity; particles engulfed	[59]
	polyethylene glycol (MW: 400 - 10,000; viscosity: 1.06-1.65 10^3Pa·s)	higher molecular weight, ***decreased*** growth rate	[60]
Solute Type	0.15-0.3 M sodium chloride (NaCl)	increased ionic salt concentration, ***decreased*** growth rate	[61]
Solute Concentration	5-30wt% sucrose	increased solute concentration,	[56]
	2-6wt% carboxymethyl cellulose	***decreased*** growth rate	[60]
Viscosity	2wt% carboxymethyl cellulose (15-1012 $Pa \cdot s^n$, n = 0.95-0.77)	increased viscosity, ***slightly*** ***increased*** growth rate	[60]

rate from 0.2 to 1 cm/sec when ice is grown on a brass plate [57]. The growth rate is also dependent on currents, which can vary within water due to natural convection or to forced flow, and can limit the growth of ice in certain directions [62].

Crystal growth kinetics can affect the final structure of the solid formed. For example, when the velocity of the ice front is increased, dendrite spacing has been shown to decrease in both poly(vinyl alcohol) and ceramic scaffolds [2,63]. In addition, crystal growth is kinetically more favorable on some crystallographic planes. Thus, crystals which nucleate with a kinetically favorable growth plane along the temperature gradient, can overtake and eventually eliminate other forms of ice crystals [40,58].

Another result of favorable growth directions within the ice crystal, is a natural tendency for ice to form anisotropic structures. This fact is exploited during systems of "directional" freeze casting, which aim to produce structures which are often have aligned pores [64]. Within anisotropic structures, growth appears to proceed in two stages, each with its own growth rate [40]. Initially, as the Gibbs free energy of undercooling is transformed into crystal growth, the growth rate is extremely fast, Figure 2. Due to a lag to reestablish undercooling of the liquid, steady state growth follows. During steady state growth, lamellar crystals form, whose orientation is influenced by both the favorable crystal direction and the temperature gradient felt at the growing tip [3]. When the temperature gradient is high, crystals grow along the direction of the temperature gradient regardless of favorable crystal orientations [3]. If the ice front velocity is too low, aligned anisotropic structures do not form [65]. This evolution is reflected macroscopically in crystal structures. The initial stages of growth are characterized by two or more crystal orientations competing with a lamellar structure, oriented parallel to the temperature gradient, eventually dominating, Figure 2 [3,40]. The transition volume, where crystal orientations compete, is determined by the initial volume in which ice growth occurs and is thus increased with increasing nucleation temperature [44]. While growth kinetics played a role, other factors could also contribute: efficiency of solute exclusion from each orientation, residual stress distributions, and the nature of the external thermal gradient [40].

3.2 Ice Crystal Growth within Solutions

As a self-cleaning structure, solute does not get incorporated into the ice crystal lattice at a high rate [1]. However, even when solute is not incorporated into the structure, the grain structure can change depending on the solute and freezing conditions of the aqueous solution [34,66]. When polymeric solutes are present, dendrites form, due to perturbations in the solid-liquid interface [54]. As the initial polymer concentration increases within the solution, dendrite branches coarsen [66]. When the concentration of solutes is low enough and freezing is rapid, irregular dendrites, whose thickness is affected by solute concentration, predominate [66–68]. Within alumina powder slurries, additional solutes, such as gelatin, changed the structure from

lamellar to cellular, and additives such as sodium chloride could increase surface roughness [5]. Rapid freezing can cause dendrite formation. However, if the ice growth velocity is fast enough, dendritic structures can break down, allowing solutes to become entrapped in the solid rather than excluded to the inter-dendritic region [59]. In addition, when particle size or concentration increases, the likelihood of entrapping solutes, rather than excluding them, also increases. For example, in a study on freeze-casting titanium particles, when the particle diameter increased from 45 μm to 125 μm, the particles were engulfed within the growing crystal [59].

Solutes can change the rate of crystal growth in several ways. Some ionic salts have been found to slow the kinetics of crystal growth by interfering with the ordered crystal structure [61]. Others, like sucrose and polymers, slow crystal growth as the concentration increases [56, 60]. Work done with carboxymethyl cellulose (MW 80,000), showed that an increase in concentration from 0 - 5 wt% had a large impact on the linear growth rate of ice, which was not due to the increase in viscosity [60]. In addition to polymer concentration affecting crystal growth, the molecular weight of the polymer also played a role in crystallization [60]. Increasing the molecular weight of polyethylene glycol solutions, from 400-10,000 g/mol, significantly reduced the growth rate of ice. However beyond 10,000 g/mol, the molecular weight ceased to impact ice propagation [60]. Given the minimal effects of viscosity alone on the growth rate, even with a 500 times increase, polymer chains are believed to slow ice growth by mechanical hindrance of the ice crystals [60].

Not only can polymers slow crystal growth, but in some cases, they can interact with water molecules to impact the solidification behavior. Collagen, a natural polymer which has a close association with water molecules, has been shown to retain a liquid like layer around it at all times, even to -50 °C [69]. It is hypothesized that the freezing point of the water is lowered by being trapped in the very small spaces within the collagen structure, leaving 0.6g of water unfrozen per every gram of collagen fiber in solution [69].

3.3   Crystal Structure Changes over Time

During solidification, after the initial structure is formed, further remodeling can occur. Surface and bulk diffusion of molecules has been demonstrated within a wide variety of systems, not only ice [70]. The results of molecular movement are rearranged crystals and particle sintering due to plastic flow caused by the stress of inter-facial tensional forces [71].

There are three broad categories of molecular movement: attrition processes, agglomeration, and Ostwald ripening [72]. Attrition is a mechanical process, where pieces of existing ice crystals are broken apart and moved within the solution to serve as secondary nucleation sites [33]. During agglomeration, smaller particles fuse together to create a few large particles [37]. The agglomeration process only occurs at longer time points, of greater than 1 hour, and requires a non-homogeneous particle size at initiation; very small, uniformly sized particles in solution,

or high solute concentrations where no large ice particles form during nucleation, did not allow agglomeration to occur [37]. The solute itself did not appear to be incorporated within the particles, but was only absorbed on the outermost surface layer during the process [37]. The macroscopic effect of Ostwald ripening is the growth of large crystals at the expense of smaller crystals, Figure 6, due to a drive to reduce both the chemical potential of small radii of curvature and the inter-facial energy within the system [33, 38].

Ostwald ripening can be called recrystallization or even annealing in various branches of literature. Within this discussion, "Ostwald ripening" will refer to the phenomenon of large crystals growing at the expense of smaller crystals and "annealing" is defined as a change to the overall crystal structure. Also, to avoid ambiguity, the term "thermal hold" will be applied to any heat treatment with the aim of changing the crystal structure at a constant temperature.

While attrition and agglomeration processes can be avoided, Ostwald ripening always occurs to some degree during freezing. The coarsening of the ice structure occurs at temperatures which are above the glass transition temperature: the temperature below which molecular mobility becomes limited in solutions [46]. The glass transition temperature of aqueous solutions is dependent on the concentration and type of solute. Solutions of 30 wt% sucrose have glass transition temperatures below - 30 ℃, while 10 wt% hydroxyethyl starch solutions have transition temperatures above -15 ℃ [46, 73, 74]. Annealing of ice structures has been demonstrated in ice as high as -1 °C [75]. At these relatively high temperatures, small crystals are above their equilibrium temperature and dissolve, while larger crystals, below their equilibrium freezing temperature, remain [72]. In order to maintain the equilibrium between liquid and solid within the system, some of the liquid solidifies on the surface of larger ice particles, as the nucleation of new nuclei is thermodynamically unfavorable [33, 46]. The ice crystal volume increases linearly with time, and some effort has been made to model the effects of Ostwald ripening on ice crystals in solution [76, 77].

Annealing is often believed to be a mixture of more than one mechanism [78]. Where the change in crystal size is fast, in the initial stages, it has been suggested that mechanisms such as agglomeration act, which then transition to the slower, diffusion controlled Ostwald ripening [78]. The intricate process of ice growth and change over time is mirrored in the melting of ice crystals which must first undergo Ostwald ripening to become a single crystal before finally transitioning to a complete liquid [79].

Ripening of ice structures is highly dependent on the solution [76, 80]. As the concentration of solute increases, the rate of Ostwald ripening decreases. This is believed to be linked to a higher resistance to mass transfer with increasing solute [72, 80]. As sucrose solutions went from 10-42% concentration, the growth rate of the crystals decreased from 2 mm/s to 0.5 mm/s [80]. Solute type also influences Ostwald ripening. It was found that sucrose solutions had a larger crystal growth rate than ethanol solutions, and also that large molecules reduce the rate of ripening [76]. The reduction in the rate of Ostwald ripening with the addition of locust
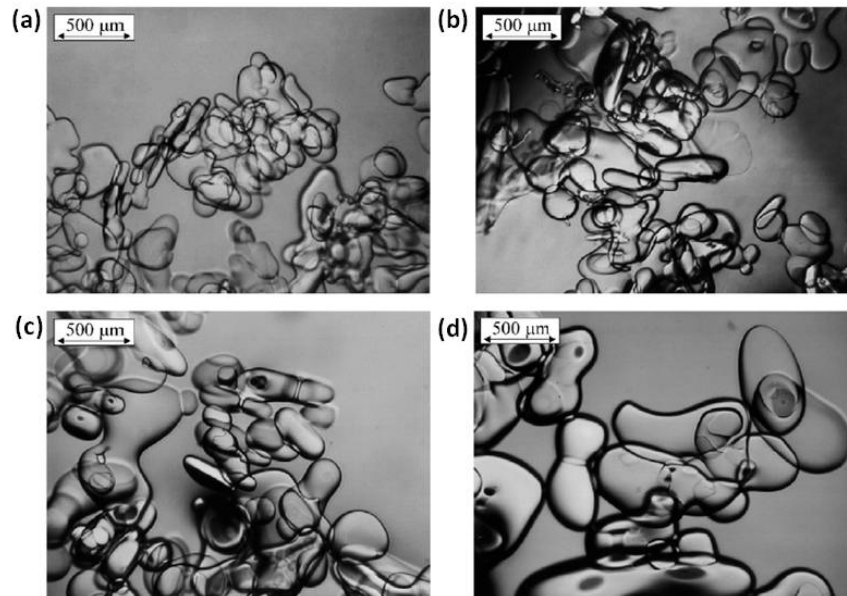
Figure 6: Ice crystals undergoing Ostwald ripening in a stirred, 4.9 wt% sodium chloride solution containing a constant 15 wt% ice after (a) 0, (b) 2, (c) 6, and (d) 22 hours [76]. Reprinted from International Journal of Refrigeration, 28(1), Pronk P, Hansen TM, Infante Ferreira CA, Witkamp GJ, Time-dependent behavior of different ice slurries during storage, 27-36, Copyright (2005), with permission from Elsevier.

bean gum, a 5000 kDa polysaccharide, was hypothesized to be caused by adsorption of the polysaccharide onto the ice surface, slowing diffusion [81]. The addition of even small amounts of polymer, up to 0.5% gelatin, decreases ice crystallization in sucrose solutions significantly [80].

Thermal holds are often used in pharmaceutical literature to both crystallize glassy mixtures and homogenize ice crystal size via induced Ostwald ripening [46]. In solutions of hydroxyethyl starch, a thermal hold of even 30 minutes above the glass transition temperature produced significant changes on the ice crystal structure, Figure 7 [46]. Being above the transition temperature dramatically increases the rate of crystal growth, although even below the glass transition temperature, crystal growth does not completely stop [73, 78]. In lamellar structures, crystals which form in the early stages of solidification are subject to coarsening over time [49]. The coarsening of the ice structure also affects dendrite spacing, which increases as crystals become thicker [3].

4 Biomedical Scaffold Structure

It has become apparent, through decades of research, that of all the tools available in regenerative medicine the supporting scaffold is one of the key factors ensuring a positive outcome by inhibiting scar formation and wound contraction [8]. Tissue engineering scaffolds act as a
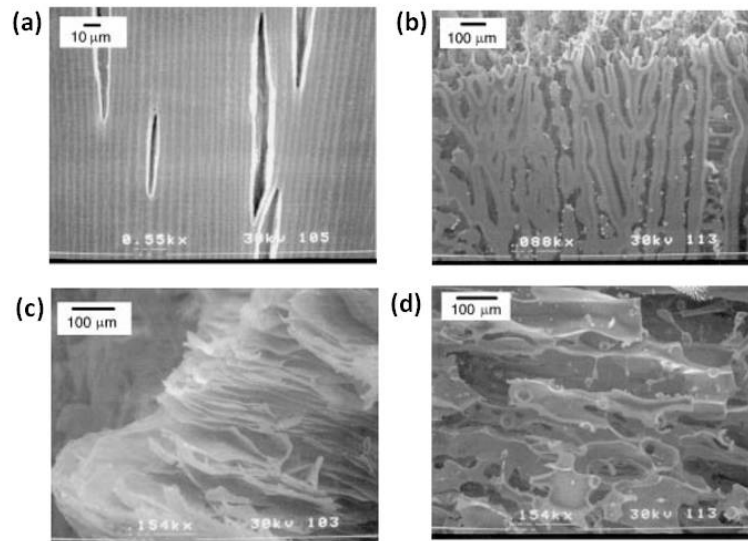
Figure 7: Thermal holds result in a significant change in structure for liquid nitrogen frozen hydroxyethyl starch solutions (10wt%). The outer top edge of the structure (a) before annealing (b) after annealing and the interior (c) before annealing and (d) annealed [46]. Journal of Pharmaceutical Sciences, Vol. 90, 872-887 (2001). Copyright 2001 Wiley-Liss, Inc. and The American Pharmaceutical Association.

framework to surround and support cells [82,83]. As constructs which mimic native extra cellular matrix (ECM), biopolymer scaffolds created from natural polymers like collagen, have been shown to be inter-connected structures which are effective as both *in vitro* models and *in vivo* repair structures [20,23]. Many properties can be varied within the scaffolds, such as chemical composition, mechanical strength, and degradation rate, to tailor the scaffolds for specific uses for systems as diverse as mammary tissue and osteochondral defects [12,20,22,23].

The structure of tissue engineering scaffolds, described by pore size and architecture, has a direct impact on biological response [8]. The structure must be able to allow nutrient diffusion and cell migration throughout the scaffold. The ideal pore size varies between cell types, but the lower limit on pore size remains relatively constant at 10-50 μm in diameter [84]. In addition to a defined pore structure, architectural cues allow biomedical scaffolds to mimic complex tissue architecture, and in the process influence cellular morphology and phenotype. In the case of tendon, a tissue organized into bundles of aligned collagen fibers, scaffolds with aligned fibers consistently promote greater cell elongation, Figure 8, and up-regulation of tenogenic markers, such as scleraxis and tenomodulin, when compared to un-aligned fibers [10,85].

As the structure of ice-templated scaffolds is formed during the freezing stage, scaffold structure is heavily dependent on all of the parameters which affect ice growth. Changes to set freezing protocols are known to affect scaffold architecture radically. Many different variables can be adjusted independently, including: set freezing temperature, set cooling rate, and thermal holds. While the principle of ice-templating is the same, there are a variety of techniques for freezing the slurry. In the majority of tissue engineering scaffold systems, the set freezing
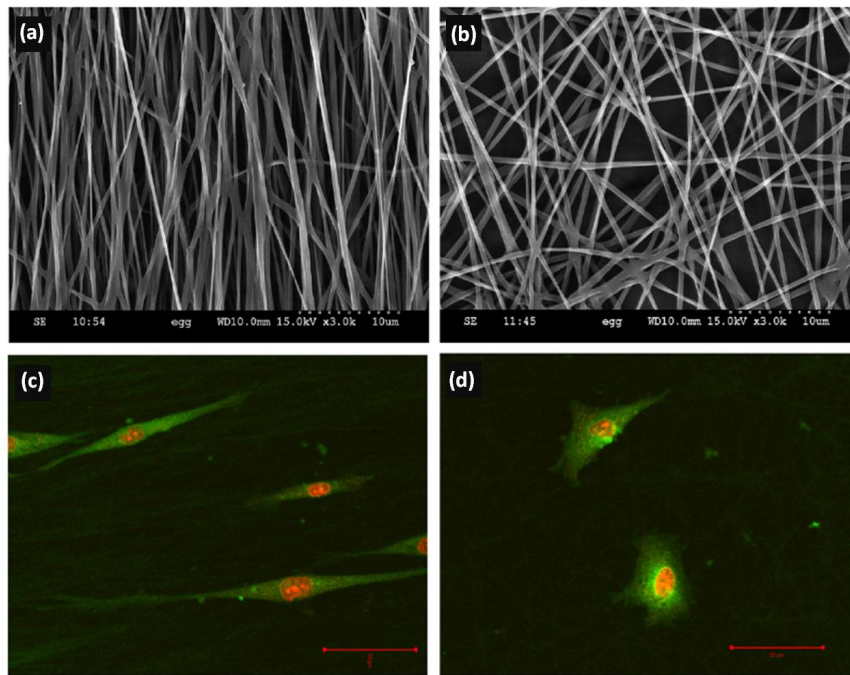
Figure 8: The fiber orientation of electrospun poly(L-lactic acid) influenced the morphology of human tendon stem/progenitor cells. On (a, c) aligned scaffolds, cellular morphology was elongated. On (b, d) randomly oriented scaffolds, cells were not elongated. Scale bar in (a, b) 10μm, (c, d) 50μm; red was nuclei, green was cytosol [25]. Reprinted from Biomaterials, 31(8), Yin Z, Chen X, Chen JL, Shen WL, Nguyen TMH, Gao L, Ouyang HW, The regulation of tendon stem cell differentiation by the alignment of nanofibers, 2163-2175, Copyright (2010), with permission from Elsevier.

temperature is often dictated by the method used to cool the suspension, such as cooling in liquid baths, quenching in liquid nitrogen, or placement in freezers [52, 86]. A shelf-ramping freeze drier is one of the most versatile methods of freezing, which allows both the set freezing temperature and the set cooling rate to be varied independently [52]. Due to the variety of techniques used to freeze scaffolds prior to lyophilization, it is often difficult to separate the effect of set cooling rate and set freezing temperature of the system. However, both the set cooling rate and set freezing temperature have been shown to influence the scaffold structure.

4.1   Change in Scaffold Architecture with Set Freezing Protocol

The Effect of Set Cooling Rate

Very fast cooling, such as quenching, can shift where nucleation occurs [86, 87]. This has been demonstrated in systems with natural polymeric materials (alginate and cellulose), cooled to -80 °C, where the pore structure changed from isotropic at a cooling rate of 0.83 ºC/min to an aligned architecture when quenched to -80 °C [86]. In another case, silk fibroin scaffold architecture changed from equiaxed to lamellar when the freezing protocol changed from quenching at -20 °C to a quench at -73 °C [87]. In both cases, the cooling rate had the power to change where nucleation and the initial fast crystal growth occurred within the sample volume and resulted in a shift from isotropic to anisotropic structure. Studies such as these support the hypothesis that there exists a critical cooling rate for each system, below which the initial equiaxed crystal growth occurs only within a small region [41]. However, it must be noted that the set cooling rate applied to the slurry is not necessarily the cooling rate of the slurry itself [88, 89]. It is often the mold which mediates how the slurry is cooled, and thus, also affects the scaffold architecture [28, 90].

The effects of moderate set cooling rates, from 0.6 - 4.1 °C/min, have been examined in collagen scaffolds [91]. Decreasing the set cooling rate of a 0.5 wt% collagen suspension reduced the pore size. The homogeneity of the structure was also altered, with a set cooling rate of 0.9 °C/min leading to the greatest scaffold homogeneity [91].

Effect of Set Freezing Temperature

Set freezing temperature also has a direct impact on scaffold structure, independent of set cooling rate. When the set freezing temperature of a 0.5 wt% collagen suspension was decreased from -10 to -40 °C, holding the set cooling rate at 1.4 °C/min, it was observed that the scaffold pore size decreased from 150 μm to 100 μm, Figure 9 [88]. When the set freezing temperature of the collagen slurry exceeded -50 °C, the pore size remained constant at around 90 μm pores [89]. It was shown that at -42 °C, using differential thermal analysis, that the collagen
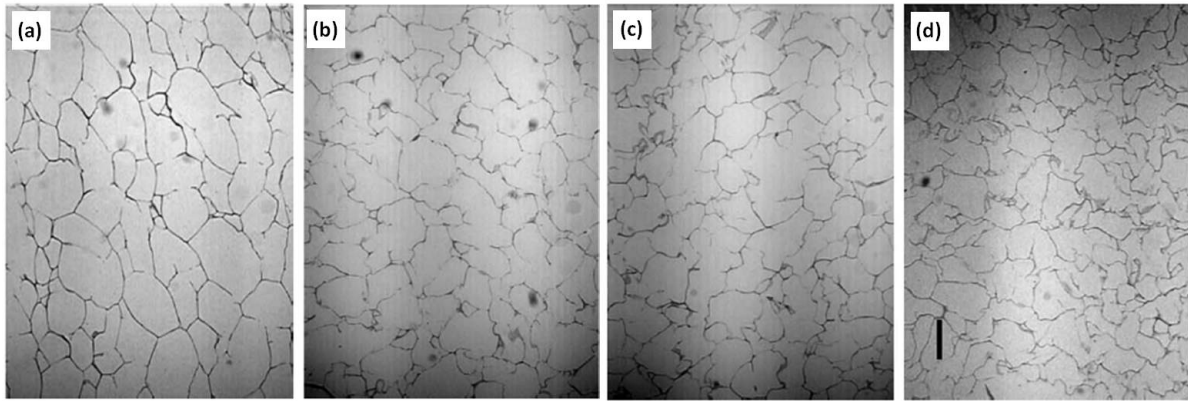
Figure 9: Micrographs of collagen-GAG scaffolds with set freezing temperature of (a) -10°C, (b) -20°C, (c) -30°C, (d) -40°C [88]. Scale bar: 100 µm. Reprinted from Biomaterials, 26(4), O'Brien FJ, Harley BA, Yannas IV, Gibson LJ, The effect of pore size on cell adhesion in collagen-GAG scaffolds, 433-441, Copyright (2005), with permission from Elsevier.

slurry underwent a glass transition, increasing the viscosity of the solution and limiting the diffusion of molecules, and thus limiting growth of ice crystals [89]. It has been theorized that the influence of set freezing temperature, independent of set cooling rate, stems from the temperature difference seen by the suspension after primary nucleation, when the rejection of latent heat has raised the temperature of the sample back to its equilibrium freezing temperature [92]. If the temperature difference between the equilibrium freezing temperature and the set freezing temperature is large enough, freezing can be completed rapidly. If the set freezing temperature is high, freezing time will increase, possibly allowing annealing of the pores to occur after the initial nucleation event [41].

Addition of a Thermal Hold

Set cooling rate and set freezing temperature are not the only steps in set freezing protocols which can be altered. Adding a thermal hold to the freezing cycle changes the pore size and also improves the overall homogeneity of the pore structure, as the system attempts to reduce the inter-facial energy [39]. At higher temperatures and after longer time periods, the effects of the thermal hold on annealing are increased [39, 89]. An investigation of a thermal hold on the pore size of 0.5 wt% collagen scaffolds found that the maximum pore size was reached at 18 hours, after which no further increase was recorded [89]. Not only can the pore size be changed with longer periods at the set freezing temperature, but the isotropy of a scaffold can be altered. After being held for 16 hours at -20 °C, it has been observed in frozen chitosan solutions that ice architecture changed from equiaxed, interconnected porosity to lamellar and largely disconnected pores [93]. The change in structure was hypothesized to be due to temperature gradients within the system which could cause certain crystal directions to grow favorably as smaller ice crystals were dissolved.

4.2   Relating Scaffolds to the Physics of Solidification

Changes to set freezing protocol are a powerful way to tailor biopolymer scaffold architecture. In addition, a large number of other variables can be altered during the ice-templating process, including solute concentration and macroscopic aspects of production, such as slurry height and mold design [29, 90]. Underlying all of the different variables within biomedical scaffold production, are the fundamental physics of ice nucleation and growth. In order to relate the changes in scaffold architecture with set variables to ice solidification, it is first necessary to observe how the ice freezes within the slurry. Using thermal profiles, a record of the freezing events can be obtained, and from that, the behavior of ice nucleation and growth can be described in terms of the slurry cooling rate, the nucleation temperature, and the freezing time, Figure 10. It is important to note that the freezing behavior of an entire volume of slurry cannot be defined by one point within the slurry, except in cases when the slurry volume is small enough that no internal temperature gradients will exist. As seen in Figure 10, freezing parameters, such as the slurry cooling rate, change continuously within the slurry volume and are also distinctly different from the set freezing parameters which can be externally controlled [29].
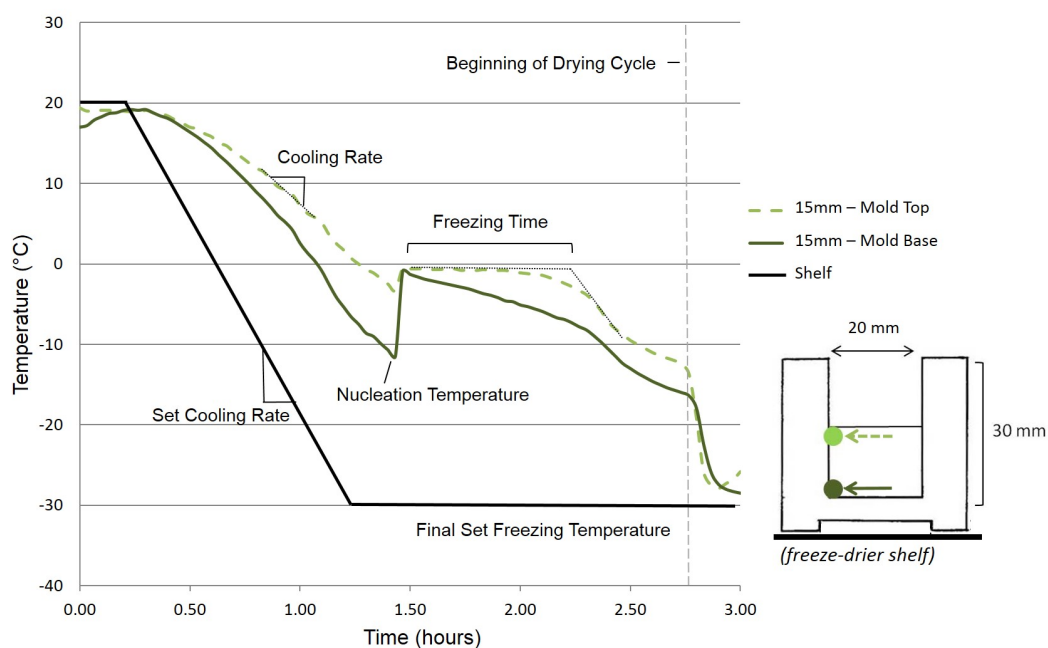

Figure 10: An example of a thermal profile of a 1 wt% collagen slurry taken during freezing, and the way in which it can be used to quantify thermal parameters and describe ice growth. The thermal events within the slurry cannot be described by the set freezing parameters, which can be controlled during freezing. The freeze-drying mold, in the schematic, is made from perspex and was cooled from the base by the freeze-drier shelf [29]. Adapted from Materials Science and Engineering C, 37, Pawelec KM, Husmann A, Best SM, Cameron RE, Understanding anisotropy and architecture in ice-templated biopolymer scaffolds, 141-147, Copyright (2014), with permission from Elsevier.

The variations in solidification behavior of the slurry with changes in slurry volume and height have been shown to have profound affects on the freezing of ice and the final structure of the scaffolds created [29] In general, as the volume of slurry decreases, the nucleation temperature decreases as well and the resulting structures are more homogeneous [38, 39]. For example, increasing the slurry volume from 1 to 1.7 ml of 5 wt% bovine serum albumin was shown to increase the nucleation temperature from -8.9 to -5.3 ℃ [39]. This principle can be extended to describe the formation of anisotropic structures [29]. While anisotropic scaffold architectures are most commonly related to high set cooling rates, it has been found that anisotropy is dictated by the local temperatures within the slurry volume at the time when primary nucleation occurs [29]. If areas of the slurry are above the equilibrium freezing temperature, then no ice can form within that portion of the slurry volume during the events at primary nucleation, which involve the formation and rapid growth of ice crystals [29]. Thus, the key to creating anisotropic structures is to vary the cooling within the slurry so that, when nucleation occurs, only a small portion of the volume will be below the equilibrium temperature. Conditions conducive to anisotropic scaffold architecture can be accomplished in several ways. Increasing the filling height of the slurry, and thus decreasing the cooling rate at the slurry top relative to the base, is one simple way to induce scaffold anisotropy [29].

Another important factor which influences scaffold architecture is the mold design, which can affect both the nucleation and growth of ice independently [90]. Mold design affects when and where ice nucleates within a collagen slurry, which dictates the scaffold architecture and homogeneity of the final structure [28, 90]. Even changing the diameter of a mold from 4 to 7 mm, keeping the slurry height the same, can change the pore size at the end of solidification [39]. Anisotropic structures result when mold designs induce an internal temperature gradient within the slurry during the cooling stage prior to nucleation. This can be done by incorporating materials with a large difference in thermal diffusivity from the slurry, such as stainless steel or copper [90]. After nucleation occurs, the mold can still alter the scaffold structure by limiting the conduction of heat out of the slurry and allowing ice crystals more time to grow. Changes in the contact area with the heat sink have been shown to alter the efficiency of heat removal, thus affecting the range of pore sizes within the scaffold, and therefore the scaffold heterogeneity [90].

Despite the plethora of independent variables which can alter scaffold structure, it has recently been shown that the key to predicting the final pore size of isotropic structures is related to the annealing of ice crystals during solidification [30]. Ostwald ripening has been shown to occur within solidifying collagen slurries, causing changes in pore size even before the end of solidification. A parameter termed the "time at equilibrium" or the amount of time which the slurry spends around the equilibrium temperature, when ice has the fastest annealing potential, has been found to be a good predictor of scaffold pore size, Figure 11. The longer the slurry spends near the equilibrium temperature, either through the use of higher set freezing temperatures or

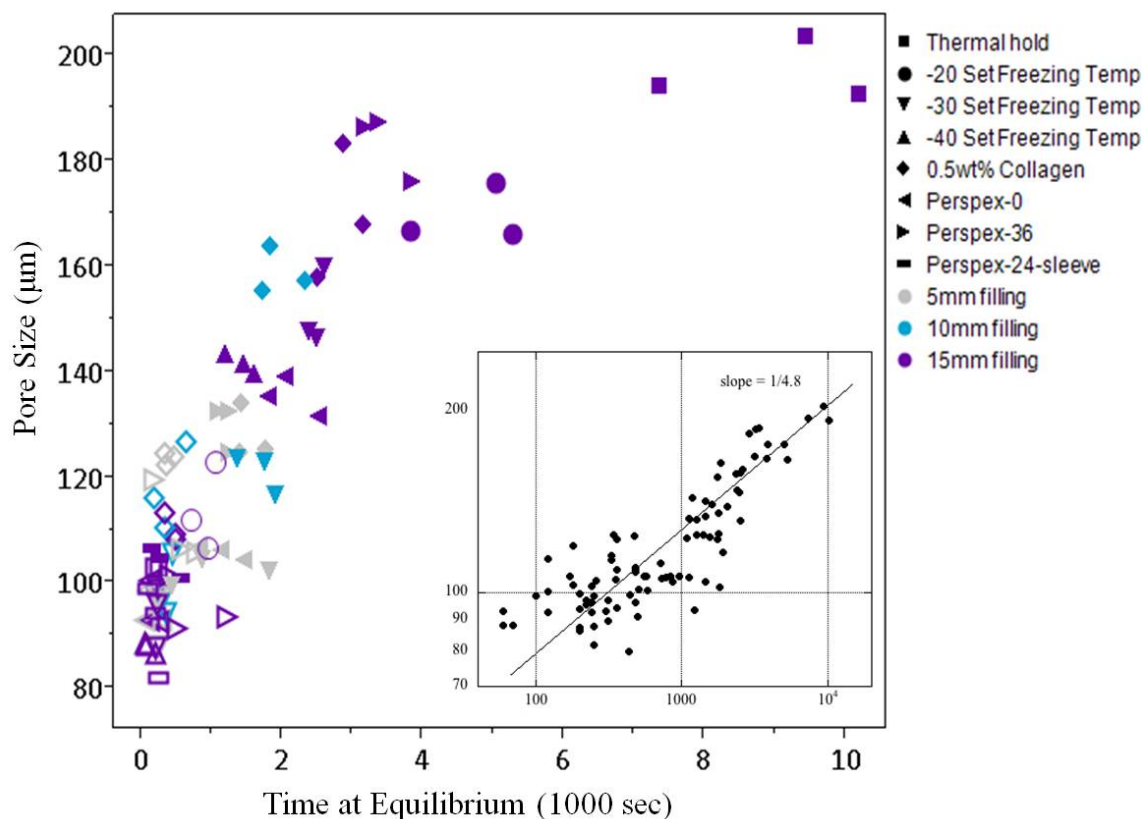## Relationship Between Pore Size and Time at Equilibrium

Figure 11: The final pore size of an ice-templated collagen slurry is dependent on the amount of time spent near the equilibrium freezing temperature, which encourages crystal growth and annealing of the structure. Inset: pore size and time at equilibrium were related by a power of 4.8, fit with a linear regression curve ($p < 0.05$, $R^2 = 0.8$). Closed markers: measurements at the top of slurry, open markers: base of slurry; colors correspond to filling height of the slurry [30]. Adapted from J. R. Soc. Interface 11, 20130958, copyright 2014, with permission from The Royal Society.

the addition of thermal holds to the freezing protocol, the pore size increases due to annealing. The relationship was robust, even when the set freezing protocol, slurry composition, mold design and filling height in the mold were altered [30].

All of the individual pieces which are known about how the physics of ice solidification influence scaffold pore structure, make a powerful set of design protocols for researchers, Figure 12. Not only can the anisotropy of the scaffold be controlled, but the pore size as well. By relying on an underlying physical principle, researchers can tune scaffold structures to their specific needs, and thus tune the biological properties of that scaffold as well. Given the broad applicability of ice-templating to so many systems, a design protocol such as Figure 12, could form a guideline for use with many materials systems and inform the many branches of science which rely on ice-templated structures. With so many variables which can be altered to tailor the ice-templating structure, there remain many avenues for continued exploration to usher in
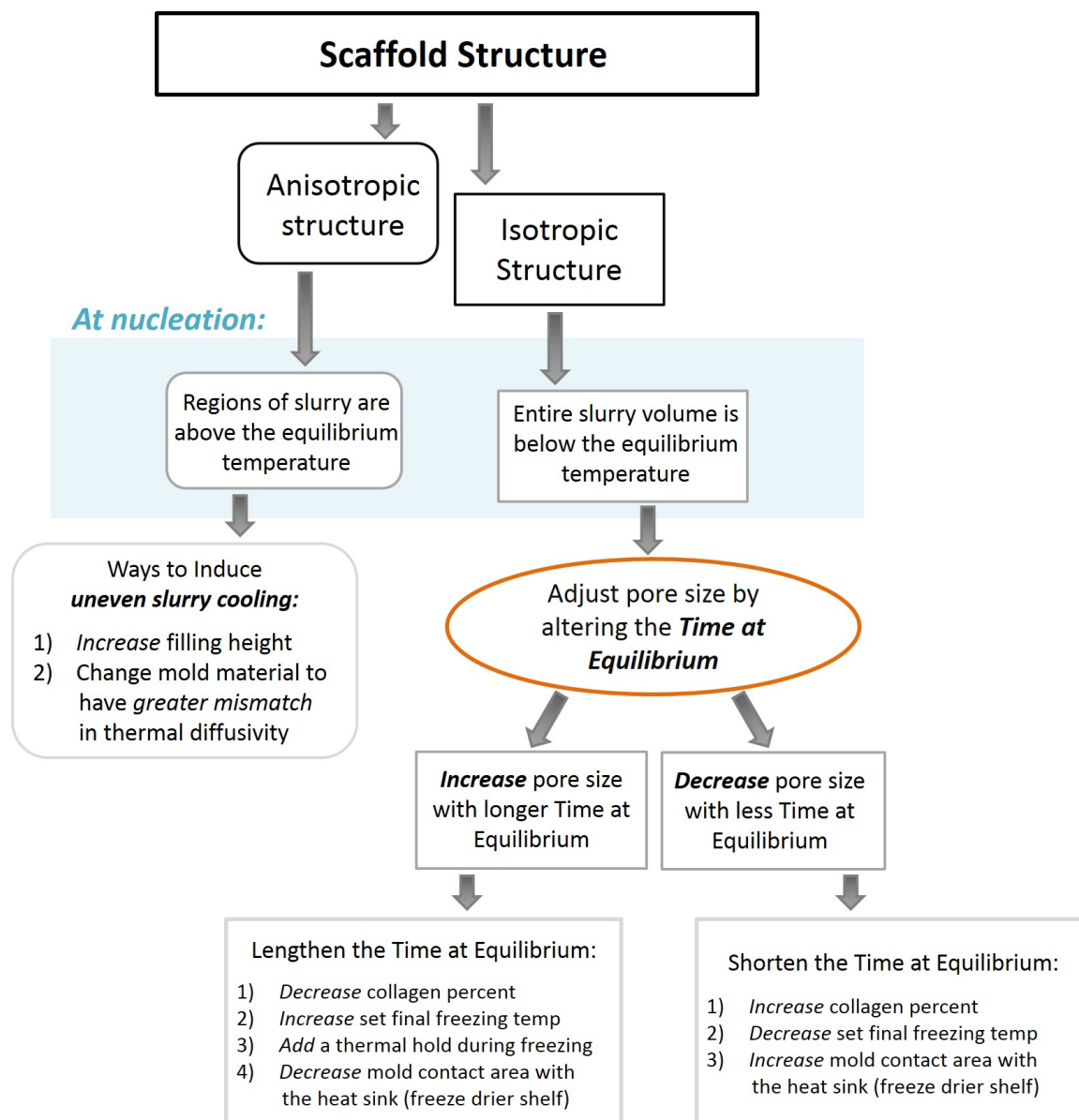
Figure 12: A flow chart summarizing the key points to creating scaffold structure and ways in which to alter the processing to tailor the scaffold structure [30]. Adapted from J. R. Soc. Interface 11, 20130958, copyright 2014, with permission from The Royal Society.

a new era of well defined porous structures for medical and engineering applications.

5 Conclusion

Ice-templating is a powerful and versatile technique which utilizes the freezing of a water-based suspension to concentrate solids into porous scaffold structures. These structures are defined by the structure of the ice which formed during solidification. This, in turn, is controlled by the physics governing ice nucleation and crystal growth. At the start of solidification, the nucleation of ice crystals, which is a stochastic process, defines the scaffold architecture, whether isotropic or anisotropic. The final features of the scaffold, such as pore size, are influenced by crystal growth. The rate of crystal growth is sensitive to the crystal orientation, solutes and freezing protocol, and the ice structure is further modified by annealing. Ice-templating has many uses, one of which is tissue engineering scaffolds, which rely on architectural cues to dictate biological responses. By looking beyond set processing conditions, and relating the physics of ice nucleation to scaffold structure, it has been found that anisotropy of ice-templated scaffolds and the final pore size and homogeneity can be predicted with the use of thermal profiles during freezing. By combining this knowledge into a set of design protocols, a new generation of tailored ice-templated structures is within reach to improve the many fields which utilize ice templating.

6 Acknowledgments

References

[1] Hobbs, P. V. *Ice Physics*. Oxford University Press, Oxford, (1974).

[2] Zhang, H. F., Hussain, I., Brust, M., Butler, M. F., Rannard, S. P., and Cooper, A. I. *Nature Materials* **4**(10), 787–793 (2005).

[3] Deville, S., Adrien, J., Maire, E., Scheel, M., and Di Michiel, M. *Acta Materialia* **61**(6), 2077–2086 (2013).

[4] Deville, S., Saiz, E., and Tomsia, A. P. *Biomaterials* **27**(32), 5480–5489 (2006).

[5] Munch, E., Saiz, E., Tomsia, A. P., and Deville, S. *Journal of the American Ceramic Society* **92**(7), 1534–1539 (2009).

[6] Zheng, J., Salamon, D., Lefferts, L., Wessling, M., and Winnubst, L. *Microporous and Mesoporous Materials* **134**, 216–219 (2010).

[7] Yoshida, S., Kimura, Y., Ogino, I., and Mukai, S. R. *Journal of Chemical Engineering of Japan* **46**(9), 616–619 (2013).

[8] Yannas, I. V. *Biomaterials* **34**(2), 321–330 (2013).

[9] Murphy, C. M., Haugh, M. G., and O'Brien, F. J. *Biomaterials* **31**(3), 461–466 (2010).

[10] Caliari, S. R. and Harley, B. A. C. *Biomaterials* **32**(23), 5330–5340 (2011).

[11] Araujo, J., Davidenko, N., Cameron, R. E., and Best, S. M. *Journal of Biomedical Materials Research Part A* (2014).

[12] Davidenko, N., Campbell, J. J., Thian, E. S., Watson, C. J., and Cameron, R. E. *Acta Biomaterialia* **6**(10), 3957–3968 (2010).

[13] Mullen, L. M., Best, S. M., Brooks, R. A., Ghose, S., Gwynne, J. H., Wardale, J., Rushton, N., and Cameron, R. E. *Tissue Engineering Part C-Methods* **16**(6), 1439–1448 (2010).

[14] Grover, C. N., Cameron, R. E., and Best, S. M. *Journal of the Mechanical Behavior of Biomedical Materials* **10**, 62–74 (2012).

[15] Grover, C. N., Farndale, R. W., Best, S. M., and Cameron, R. E. *Journal of Biomedical Materials Research Part A* **100A**(9), 2401–2411 (2012).

[16] Grover, C. N., Gwynne, J. H., Pugh, N., Hamaia, S., Farndale, R. W., Best, S. M., and Cameron, R. E. *Acta Biomaterialia* **8**(8), 3080–3090 (2012).

[17] Enea, D., Gwynne, J., Kew, S., Arumugam, M., Shepherd, J., Brooks, R., Ghose, S., Best, S., Cameron, R., and Rushton, N. *Knee Surgery Sports Traumatology Arthroscopy* **21**(8), 1783–1793 (2013).

[18] Kew, S. J., Gwynne, J. H., Enea, D., Brookes, R., Rushton, N., Best, S. M., and Cameron, R. E. *Acta Biomaterialia* **8**(10), 3723–3731 (2012).

[19] Shepherd, J. H., Ghose, S., Kew, S. J., Moavenian, A., Best, S. M., and Cameron, R. E. *Journal of Biomedical Materials Research Part A* **101A**(1), 176–184 (2013).

[20] Campbell, J. J., Davidenko, N., Caffarel, M. M., Cameron, R. E., and Watson, C. J. *Plos One* **6**(9), 9 (2011).

[21] Lynn, A. K., Nakamura, T., Patel, N., Porter, A. E., Renouf, A. C., Laity, P. R., Best, S. M., Cameron, R. E., Shimizu, Y., and Bonfield, W. *Journal of Biomedical Materials Research Part A* **74A**(3), 447–453 (2005).

[22] Lynn, A. K., Best, S. M., Cameron, R. E., Harley, B. A., Yannas, I. V., Gibson, L. J., and Bonfield, W. *Journal of Biomedical Materials Research Part A* **92A**(3), 1057–1065 (2010).

[23] Getgood, A. M. J., Kew, S. J., Brooks, R., Aberman, H., Simon, T., Lynn, A. K., and Rushton, N. *Knee* **19**(4), 422–430 (2012).

[24] Biewener, A. *Tendons and Ligaments: Structure, Mechanical Behavior and Biological Function*, book section 10, 269–284. Springer, New York (2008).

[25] Yin, Z., Chen, X., Chen, J. L., Shen, W. L., Nguyen, T. M. H., Gao, L., and Ouyang, H. W. *Biomaterials* **31**(8), 2163–2175 (2010).

[26] Pawelec, K. M., Wardale, J., Best, S. M., and Cameron, R. E. Manuscript submitted.

[27] Pawelec, K. M., Wardale, J., Best, S. M., and Cameron, R. E. In preparation.

[28] Davidenko, N., Gibb, T., Schuster, C., Best, S. M., Campbell, J. J., Watson, C. J., and Cameron, R. E. *Acta Biomaterialia* **8**(2), 667–676 (2012).

[29] Pawelec, K. M., Husmann, A., Best, S. M., and Cameron, R. E. *Materials Science & Engineering C* **37**, 141–147 (2014).

[30] Pawelec, K. M., Husmann, A., Best, S. M., and Cameron, R. E. *Journal of the Royal Society Interface* **11**(20130958) (2014).

[31] Wilson, P. W., Heneghan, A. F., and Haymet, A. D. J. *Cryobiology* **46**(1), 88–98 (2003).

[32] Deville, S. *Advanced Engineering Materials* **10**(3), 155–169 (2008).

[33] Myerson, A. and Ginde, R. In *Handbook of Industrial Crystallization,* Myerson, A., editor, chapter 2, 33–62. Butterworth-Heinemann2nd edition (2002).

[34] Akyurt, M., Zaki, G., and Habeebullah, B. *Energy Conversion and Management* **43**(14), 1773–1789 (2002).

[35] Matsumoto, M., Saito, S., and Ohmine, I. *Nature* **416**(6879), 409–413 (2002).

[36] Ayel, V., Lottin, O., Faucheux, M., Sallier, D., and Peerhossaini, H. *International Journal of Heat and Mass Transfer* **49**(11-12), 1876–1884 (2006).

[37] Shirai, Y., Sugimoto, T., Hashimoto, M., Nakanishi, K., and Matsuno, R. *Agricultural and Biological Chemistry* **51**(9), 2359–2366 (1987).

[38] Searles, J. In *Freeze-Drying/Lyophilization of Pharmaceutical and Biological Products*, Rey, L. and May, J., editors, chapter 4. Marcel Dekker, Inc., New York2nd edition (2004).

[39] Hottot, A., Vessot, S., and Andrieu, J. *Chemical Engineering and Processing* **46**(7), 666–674 (2007).

[40] Deville, S., Maire, E., Lasalle, A., Bogner, A., Gauthier, C., Leloup, J., and Guizard, C. *Journal of the American Ceramic Society* **92**(11), 2489–2496 (2009).

[41] Searles, J. A., Carpenter, J. F., and Randolph, T. W. *Journal of Pharmaceutical Sciences* **90**(7), 860–871 (2001).

[42] Chen, S. L. and Lee, T. S. *International Journal of Heat and Mass Transfer* **41**(4-5), 769–783 (1998).

[43] Deville, S., Maire, E., Lasalle, A., Bogner, A., Gauthier, C., Leloup, J., and Guizard, C. *Journal of the American Ceramic Society* **93**(9), 2507–2510 (2010).

[44] Lasalle, A., Guizard, C., Leloup, J., Deville, S., Maire, E., Bogner, A., Gauthier, C., Adrien, J., and Courtois, L. *Journal of the American Ceramic Society* **95**(2), 799–804 (2012).

[45] Bigg, E. K. *Proceedings of the Physical Society of London Section B* **66**(404), 688–694 (1953).

[46] Searles, J. A., Carpenter, J. F., and Randolph, T. W. *Journal of Pharmaceutical Sciences* **90**(7), 872–887 (2001).

[47] Heneghan, A. F., Wilson, P. W., Wang, G. M., and Haymet, A. D. J. *Journal of Chemical Physics* **115**(16), 7599–7608 (2001).

[48] Chow, R., Blindt, R., Chivers, R., and Povey, M. *Ultrasonics* **41**(8), 595–604 (2003).

[49] Flemings, M. C. *Solidification Processing*. Materials Science and Engineering. McGraw-Hill Book Co, New York, (1974).

[50] Gutierrez, M. C., Ferrer, M. L., and del Monte, F. *Chemistry of Materials* **20**(3), 3505–3513 (2008).

[51] Petersen, A., Schneider, H., Rau, G., and Glasmacher, B. *Cryobiology* **53**(2), 248–257 (2006).

[52] Kasper, J. C. and Friess, W. *European Journal of Pharmaceutics and Biopharmaceutics* **78**(2), 248–263 (2011).

[53] Li, W. L., Lu, K., and Walz, J. Y. *International Materials Reviews* **57**(1), 37–60 (2012).

[54] Kurz, W. and Fisher, D. *Fundamentals of Solidification*. Trans Tech Publications Ltd., New York, 4th edition, (1998).

[55] Hallett, J. *Journal of the Atmospheric Sciences* **21**(6), 671–682 (1964).

[56] Hindmarsh, J. P., Russell, A. B., and Chen, X. D. *Journal of Crystal Growth* **285**(1-2), 236–248 (2005).

[57] Lindenmeyer, C. S., Orrok, G. T., Jackson, K. A., and Chalmers, B. *Journal of Chemical Physics* **27**(3), 822–822 (1957).

[58] Mueller-Stoffels, M., Langhorne, P. J., Petrich, C., and Kempema, E. W. *Cold Regions Science and Technology* **56**(1), 1–9 (2009).

[59] Chino, Y. and Dunand, D. C. *Acta Materialia* **56**(1), 105–113 (2008).

[60] Blond, G. *Cryobiology* **25**(1), 61–66 (1988).

[61] Vrbka, L. and Jungwirth, P. *Physical Review Letters* **95**(14), 148501 (2005).

[62] Kallungal, J. P. and Barduhn, A. J. *Aiche Journal* **23**(3), 294–303 (1977).

[63] Deville, S., Saiz, E., Nalla, R. K., and Tomsia, A. P. *Science* **311**(5760), 515–518 (2006).

[64] Zhang, H. and Cooper, A. I. *Advanced Materials* **19**(11), 1529–1533 (2007).

[65] Bareggi, A., Maire, E., Lasalle, A., and Deville, S. *Journal of the American Ceramic Society* **94**(10), 3570–3578 (2011).

[66] Luyet, B. and Rapatz, G. *Biodynamica* **8**(156), 1–68 (1958).

[67] Schoof, H., Bruns, L., Fischer, A., Heschel, I., and Rau, G. *Journal of Crystal Growth* **209**(1), 122–129 (2000).

[68] Teraoka, Y., Saito, A., and Okawa, S. *International Journal of Refrigeration* **25**(2), 218–225 (2002).

[69] Dehl, R. E. *Science* **170**(NN395), 738–& (1970).

[70] Itagaki, K. *Journal of Colloid and Interface Science* **25**(2), 218–& (1967).

[71] Jellinek, H. G. and Ibrahim, S. H. *Journal of Colloid and Interface Science* **25**(2), 245–& (1967).

[72] Pronk, P., Ferreira, C. A. I., and Witkamp, G. J. *Journal of Crystal Growth* **275**(1-2), E1355–E1361 (2005).

[73] Hagiwara, T., Mao, J., Suzuki, T., and Takai, R. *Food Science and Technology Research* **11**(4), 407–411 (2005).

[74] Goff, H. D. and Sahagian, M. E. *Thermochimica Acta* **280**, 449–464 (1996).

[75] Wilson, C. *Textures and Microstructures* **5**, 19 – 31 (1982).

[76] Pronk, P., Hansen, T. M., Ferreira, C. A. I., and Witkamp, G. J. *International Journal of Refrigeration-Revue Internationale Du Froid* **28**(1), 27–36 (2005).

[77] Madras, G. and McCoy, B. J. *Chemical Engineering Science* **57**(18), 3809–3818 (2002).

[78] Sutton, R. L., Lips, A., Piccirillo, G., and Sztehlo, A. *Journal of Food Science* **61**(4), 741–745 (1996).

[79] Johnston, J. C. and Molinero, V. *Journal of the American Chemical Society* **134**(15), 6650–6659 (2012).

[80] Smith, C. E. and Schwartzberg, H. G. *Biotechnology Progress* **1**(2), 111–120 (1985).

[81] Sutton, R. L., Lips, A., and Piccirillo, G. *Journal of Food Science* **61**(4), 746–748 (1996).

[82] Harley, B. A. C. and Gibson, L. J. *Chemical Engineering Journal* **137**(1), 102–121 (2008).

[83] Stevens, B., Yang, Y. Z., MohandaS, A., Stucker, B., and Nguyen, K. T. *Journal of Biomedical Materials Research Part B-Applied Biomaterials* **85B**(2), 573–582 (2008).

[84] Harley, B. and Yannas, I. In *Principles of Tissue Engineering,* Lanza, R., Langer, R., and Vacanti, J., editors, chapter 16, 219–238. Elsevier Academic Press, New York3rd edition (2007).

[85] Kishore, V., Bullock, W., Sun, X., Van Dyke, W. S., and Akkus, O. *Biomaterials* **33**(7), 2137–44 (2012).

[86] Yuan, N. Y., Lin, Y. A., Ho, M. H., Wang, D. M., Lai, J. Y., and Hsieh, H. J. *Carbohydrate Polymers* **78**(2), 349–356 (2009).

[87] Byette, F., Bouchard, F., Pellerin, C., Paquin, J., Marcotte, I., and Mateescu, M. A. *Polymer Bulletin* **67**(1), 159–175 (2011).

[88] O'Brien, F. J., Harley, B. A., Yannas, I. V., and Gibson, L. J. *Biomaterials* **26**(4), 433–441 (2005).

[89] Haugh, M. G., Murphy, C. M., and O'Brien, F. J. *Tissue Engineering Part C-Methods* **16**(5), 887–894 (2010).

[90] Pawelec, K. M., Husmann, A., Best, S. M., and Cameron, R. E. Manuscript submitted.

[91] O'Brien, F. J., Harley, B. A., Yannas, I. V., and Gibson, L. *Biomaterials* **25**(6), 1077–1086 (2004).

[92] Padilla, A. M., Chou, S. G., Luthra, S., and Pikal, M. J. *Journal of Pharmaceutical Sciences* **100**(4), 1362–1376 (2011).

[93] Cooney, M. J., Lau, C., Windmeisser, M., Liaw, B. Y., Klotzbach, T., and Minteer, S. D. *Journal of Materials Chemistry* **18**(6), 667–674 (2008).